

IMPACT OF CORROSION ON MINING EQUIPMENT

J. V. Pellegrino Jr.
Sr. Materials Consultant
RJ Lee Group

Corrosion and the Mining Industry

- **Corrosion impacts the mining industry by degrading expensive equipment, which increases maintenance costs, lowers productions, and influences the environment.**
- **Corrosion places a large burden on manufacturers of mining equipment because operators claim failures are related to design and/or material selection/quality.**
- **In many countries, environmental regulations require treatment of mine water before its release from mines and into local watersheds.**
- **Water treatment methods include the use of multimedia filters, UV light, water softeners, activated carbon filters and Reverse Osmosis (RO) filters.**

Overview

- **Effect of RO water on carbon steel piping**
- **Two (2) case histories showing impact of corrosion on:**
 - A. Chain splice links**
 - B. AFC Conveyor Pans**

Corrosivity of Raw Mine Water and RO Water

- Tests use twenty-four (24) 25.4 mm x 50.8 mm x 1.48 to 1.71 mm thick coupons.
- Coupons are similar in composition to ASTM A106 piping.
- Coupons were sealed in separate oxygen controlled test cells for 31 days and subjected to the following environment variables
 - RO water, raw mine water or a 10% solution of raw mine water in RO water
 - Water was circulating or stagnant
 - Coupons were either partially or fully submerged in the water
- All test cells were maintained at the same temperature, which fluctuated between 19 to 21°C.
- Test temperature and pH were checked at the same time, each day.

RO Water
Circulating (C) Stagnant (S)

Raw Mine Water 10% Raw Mine Water
C S C S



Pre-Test



Post Test

Table 1. Composition/Properties of Pre-Test and Post Test Raw Mine and RO Water.

	Unused RMW	Unused ROW	CRMW	SRMW	CROW	SROW	C10% RMW	S10% RMW
Chloride (%)	11.9	16.2	12.6	11.0	21.4	16.4	15.5	16.4
Sulfate (%)	239	<0.100	291	274	<0.100	<0.100	31.0	38.0
Conductance (µmhos)	1050	77.9	869	930	116	98.1	237	247
TDS (ppm)	679	25	515	542	41	36	112	126
pH	7.81	8.05	8.33	8.05	7.36	7.6	7.89	7.67

PS

FS



PS

FS



PS

FS



CROW

C10%RMW

CRMW



SROW

S10%RMW

SRMW



RO Water.



10% RMW.



RMW

Pre and Post Test Weight and Thickness of Test Coupons

Sample Code	Original Weight, grs.	Original Thickness, mm.	Weight Before Cleaning, grs.	Weight Change Before Cleaning, grs.	Weight After Cleaning, grs.	Weight Loss After Cleaning, grs	Average Weight Loss/set	Minimum Thickness, mm
1PS*	15.73433	1.49	15.64094	0.09339	15.23284	0.50149	0.439075	1.46
2PS	17.03348	1.60	16.98533	0.04815	16.65676	0.37672		
3FS**	16.75971	1.60	16.56456	0.19515	16.25618	0.50353	0.504635	1.52
4FS	17.00137	1.61	16.71548	0.28589	16.49563	0.50574		
5PS	17.06672	1.60	17.005	0.06172	16.94289	0.12383	0.08354	1.72
6PS	16.58803	1.61	16.52389	0.06414	16.54478	0.04325		
7FS	17.05029	1.60	16.96123	0.08906	16.92934	0.12095	0.12853	1.59
8FS	16.73981	1.63	16.65781	0.0820	16.6037	0.13611		
9PS	16.88013	1.60	17.08035	-0.20022	16.71625	0.16388	0.27451	
10PS	16.80976	1.60	16.85368	-0.04392	16.42462	0.38514		
11FS	17.11423	1.63	17.566	-0.45177	16.79745	0.31678	0.29055	1.56
12FS	17.12541	1.71	17.46178	-0.33637	16.8441	0.28131		
13PS	16.75721	1.60	16.83896	-0.08175	16.65157	0.10564	0.0963	1.57
14PS	16.69001	1.60	16.7476	-0.05759	16.60305	0.08696		
15FS	16.97799	1.61	17.06845	-0.09046	16.84149	0.1365	0.13876	1.61
16FS	16.67448	1.60	16.74139	-0.06691	16.53346	0.14102		
17PS	16.8963	1.63	17.03468	-0.13838	16.25547	0.64083	0.753675	1.47
18PS	16.97018	1.61	17.26648	-0.2963	16.10366	0.86652		
19FS	16.80115	1.60	16.94386	-0.14271	15.98016	0.82099	0.875855	1.497
20FS	17.19515	1.60	17.23036	-0.03521	16.26443	0.93072		
21PS	16.81771	1.60	16.76051	0.0572	16.69237	0.12534	0.126635	1.58
22PS	16.70085	1.61	16.64021	0.06064	16.57292	0.12793		
23FS	16.72558	1.61	16.63625	0.08933	16.5944	0.13118	0.127715	1.59
24FS	16.83818	1.61	16.74942	0.08876	16.71393	0.12425		

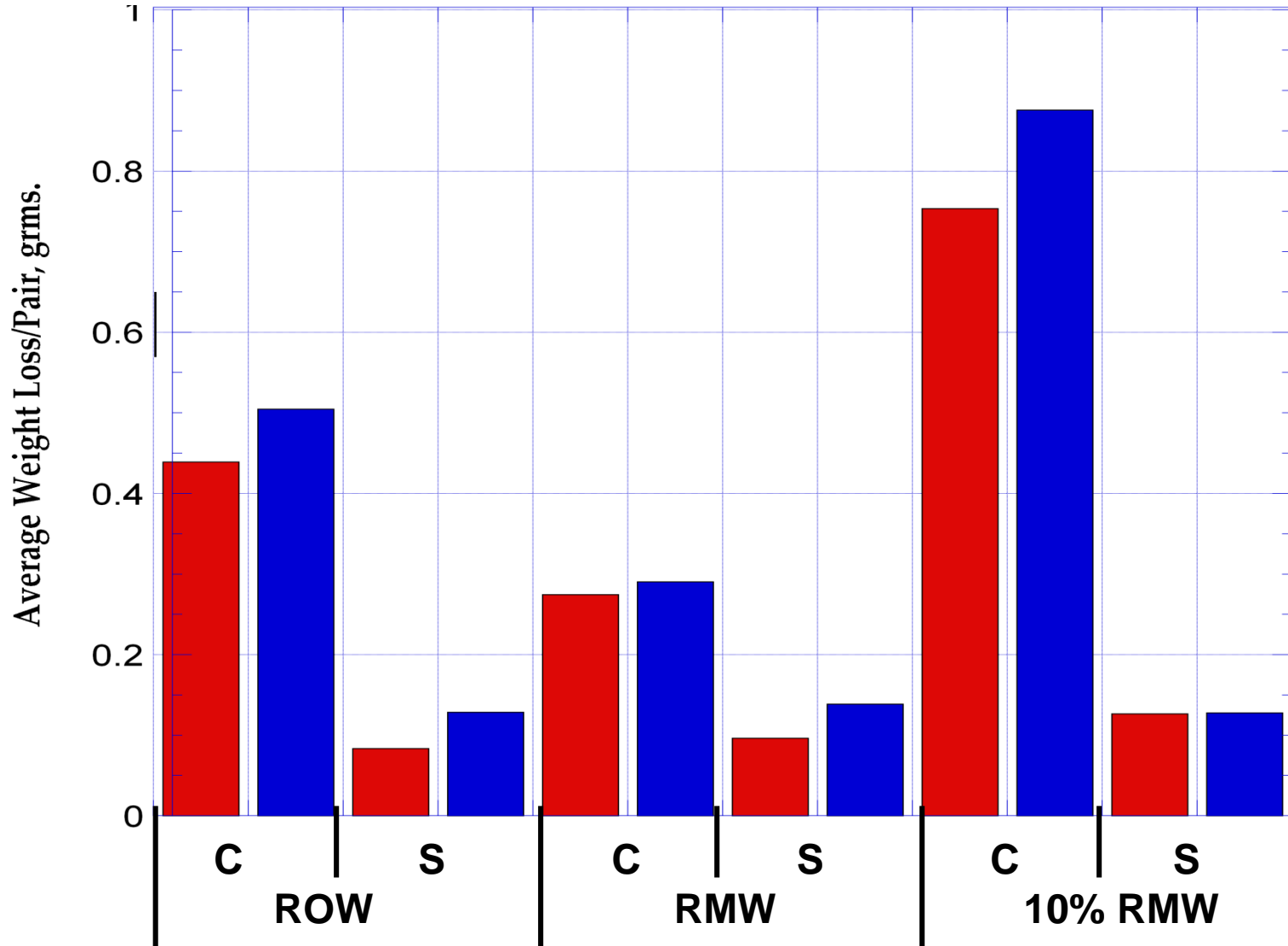
PS* - Partially Submerged

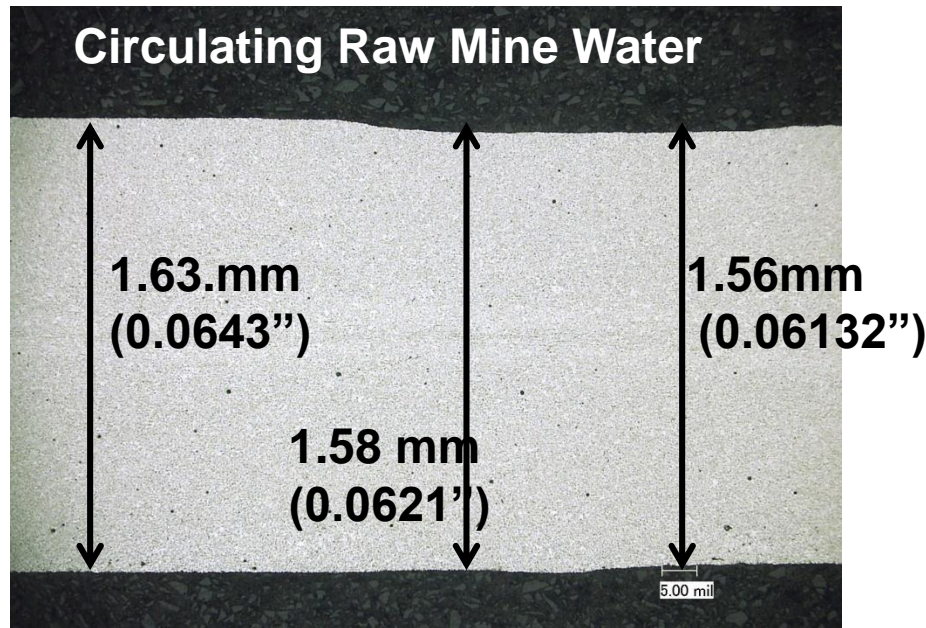
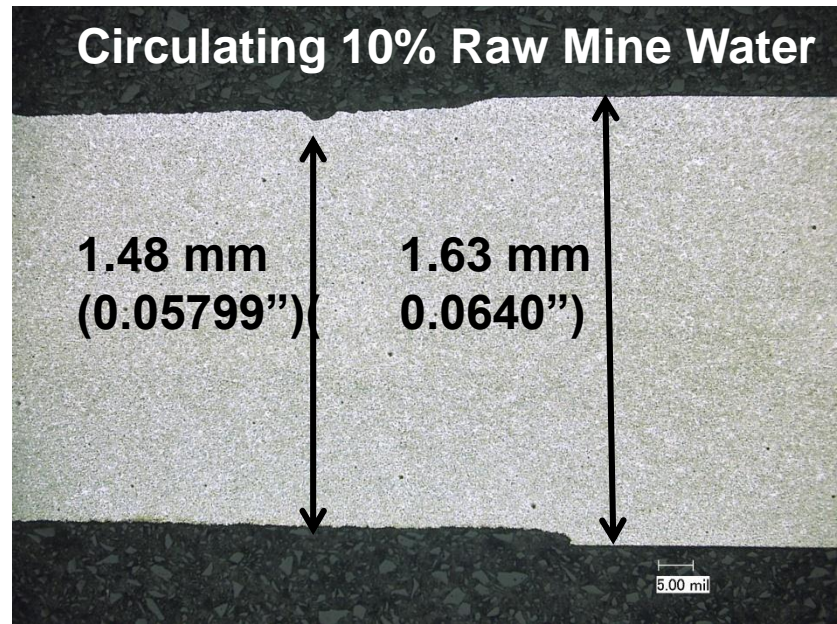
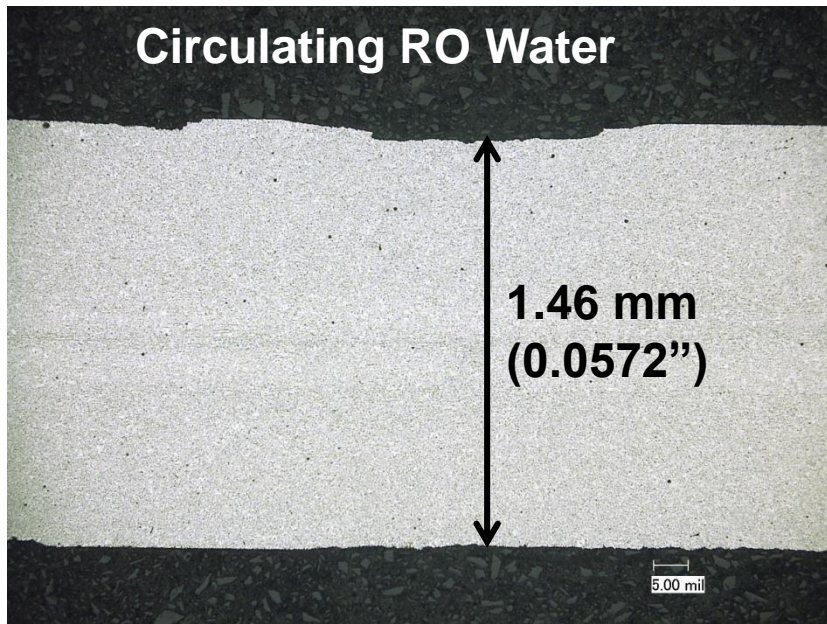
FS*** - Fully Submerged

Average Weight Loss/Pair of Partially Submerged (PS) Samples



Average Weight Loss/Pair of Fully Submerged (FS) Samples

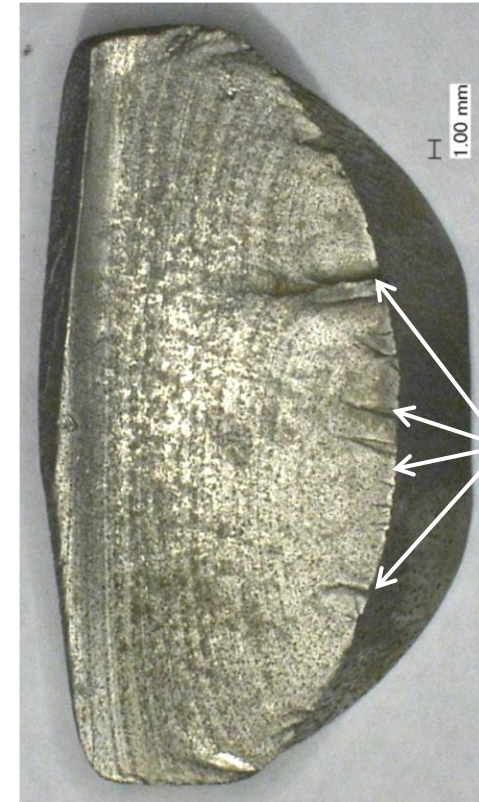
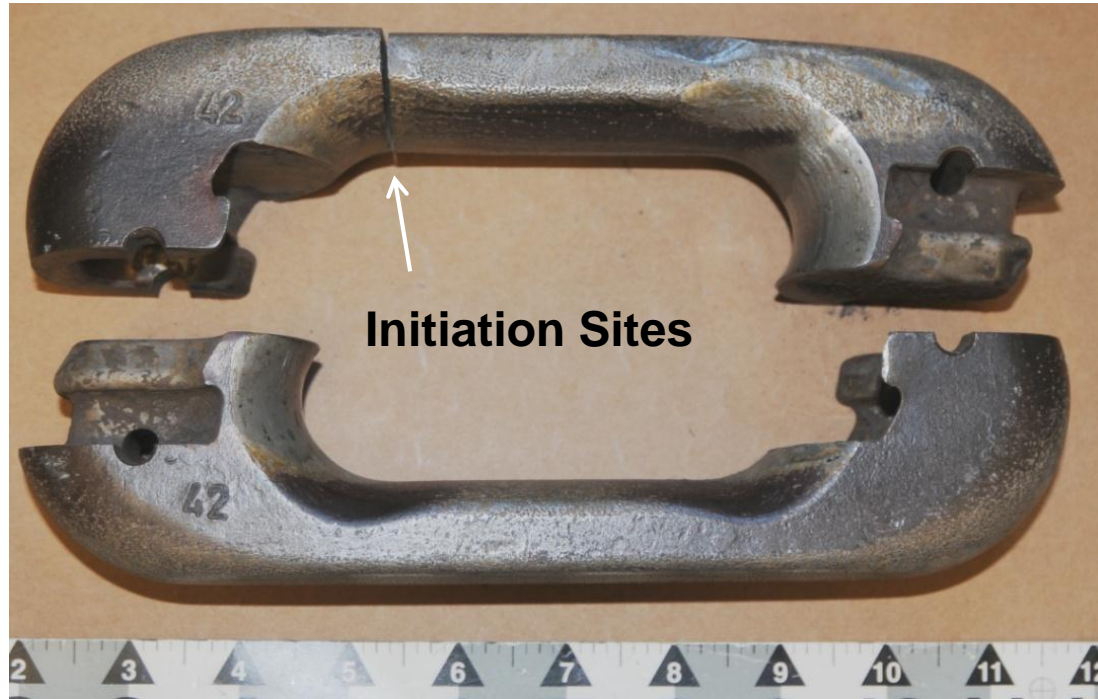




Corrosiveness of Raw Mine Water and RO Water - Summary

- Corrosion deposits heaviest on samples exposed to stagnant and circulating RO water.
- Visual examination after cleaning did not reveal the presence of excessive pitting. The uncorroded regions appeared to consist of mesas separated by relatively flat valleys.
- Samples exposed to circulating RO water and 10% raw mine water exhibited the severest corrosion.
- Difference in corrosion (weight loss) between partially submerged and fully submerged coupons was minimal.
- Under static conditions, there was no significant difference in degree of corrosion between RO treated water, raw mine water and 10% raw mine water.
- The corrosiveness of the RO treated water is primarily due to its lack of minerals and that in many cases it also contains more chlorides.

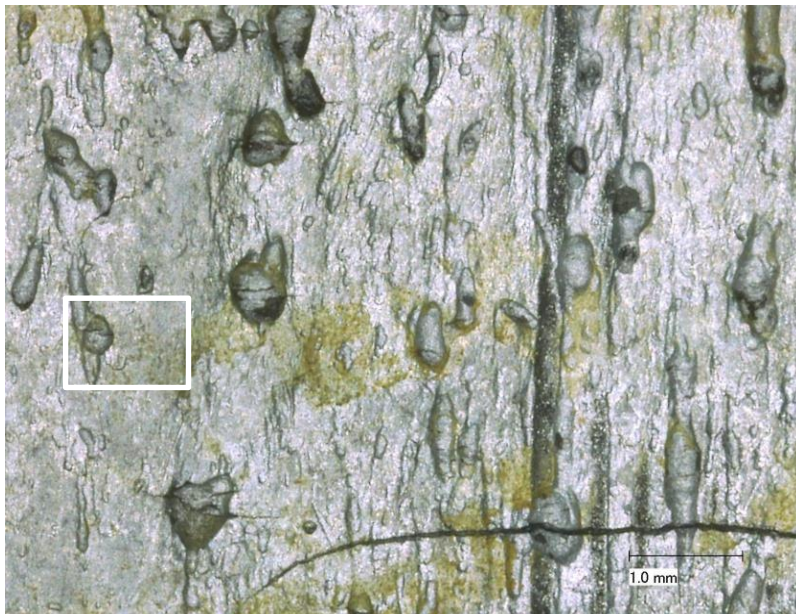
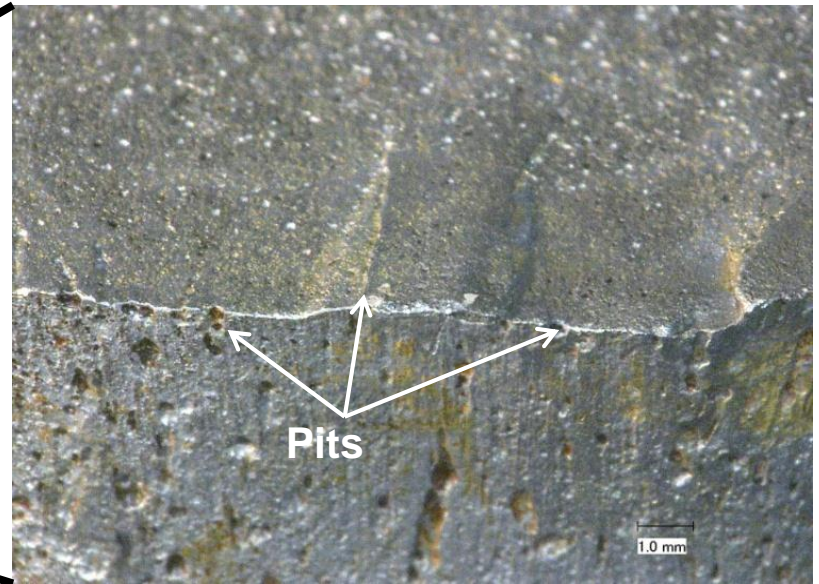
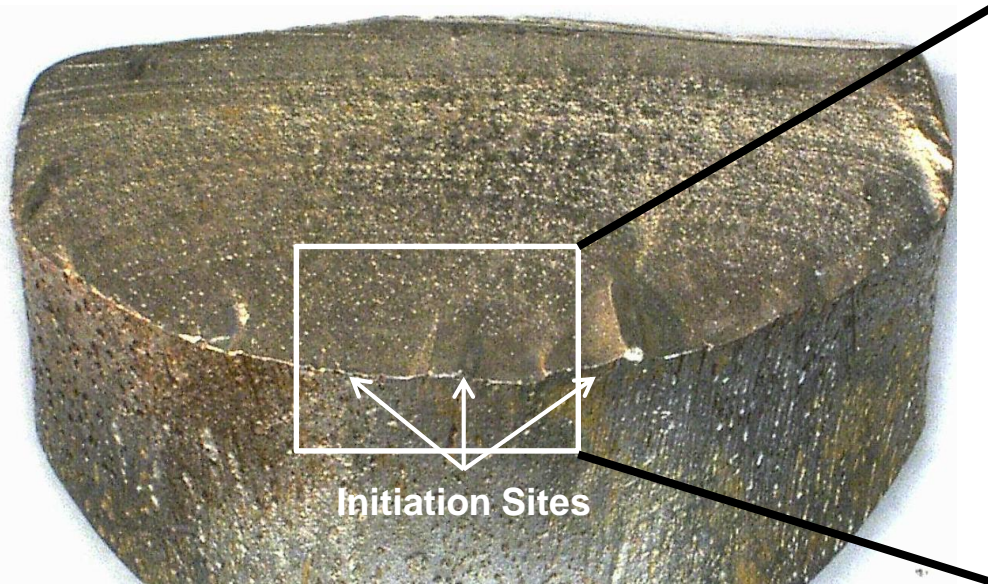
34 x 110 mm Chain Splice Link Failures

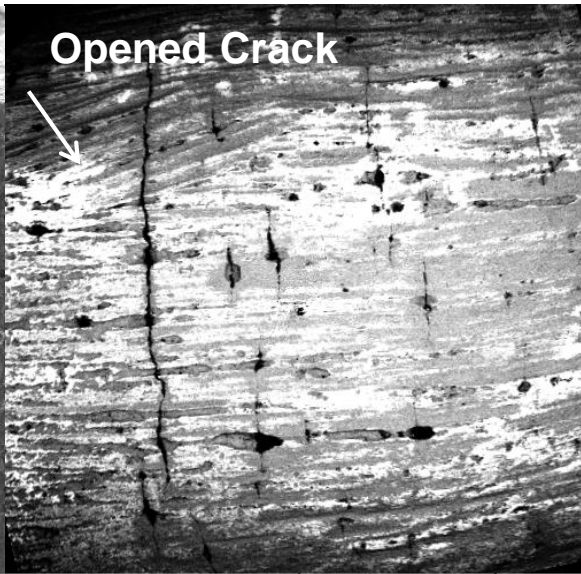
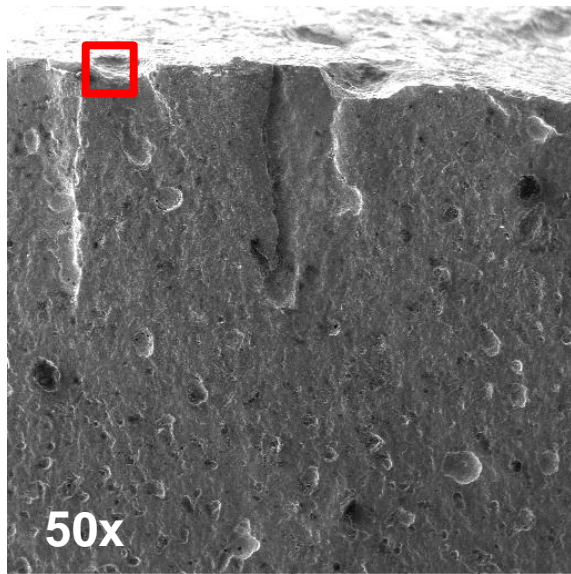


34 x 110 mm Chain Splice Link Failures Background

- Link was in service for 3 – 4 weeks.
- Used with non-galvanized standard DIN chain that had a “Tectyl” coating that exhibited satisfactory service performance.
- Alloy steel quenched and tempered to a hardness of 395 HWB (43.5 HRC)/~1337 MPa (194 ksi) and expected to exhibit a breaking load of 2000 kN (450 kips).
- Electroplated with ZnNi.

34 x 110 mm Chain Splice Link Failures



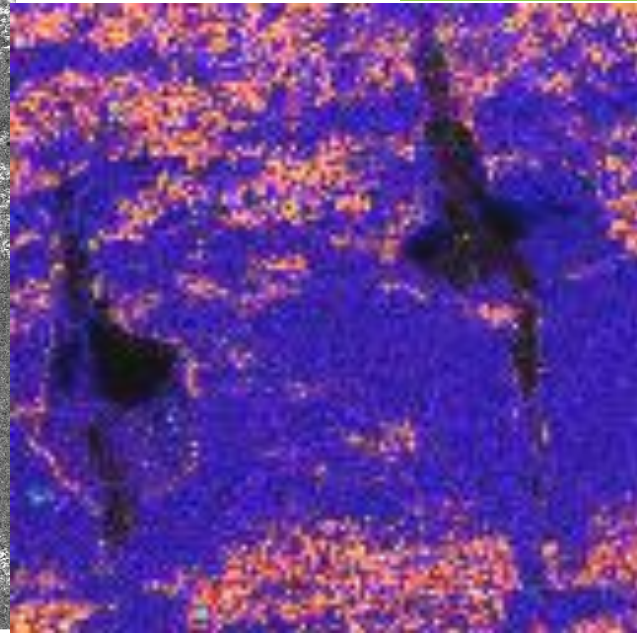
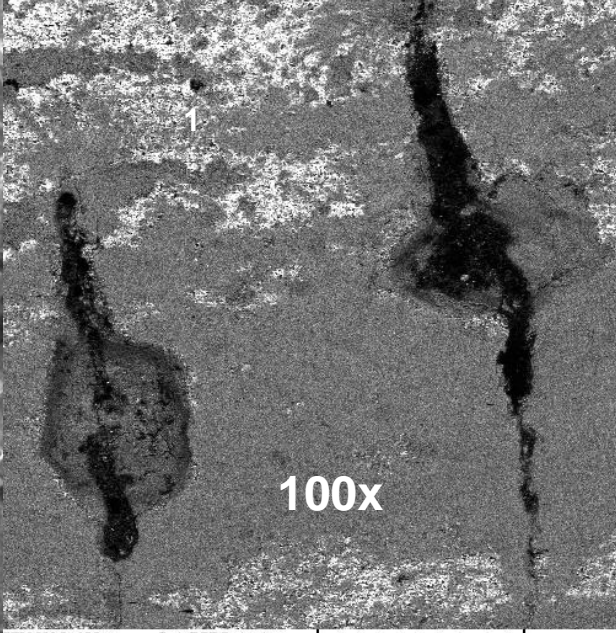
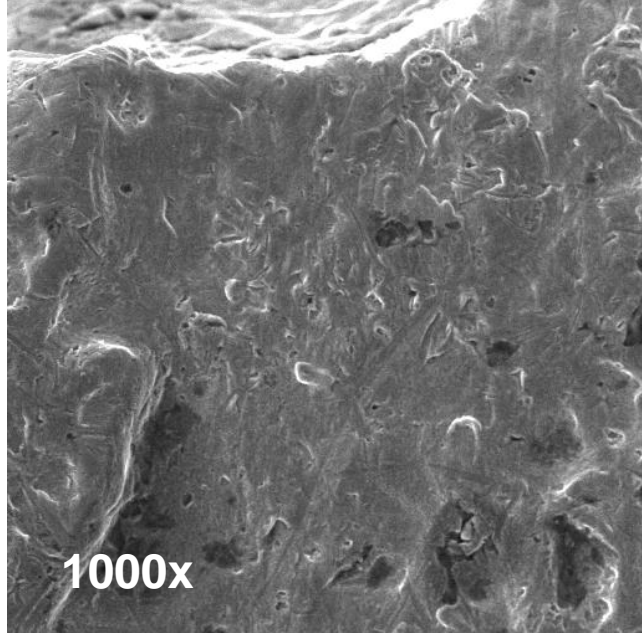


Scanning Electron Microscopy (SEM) Images

- Fe - Blue
- Zn - Red
- Ni - Yellow
- Cl - Pink
- S - Green

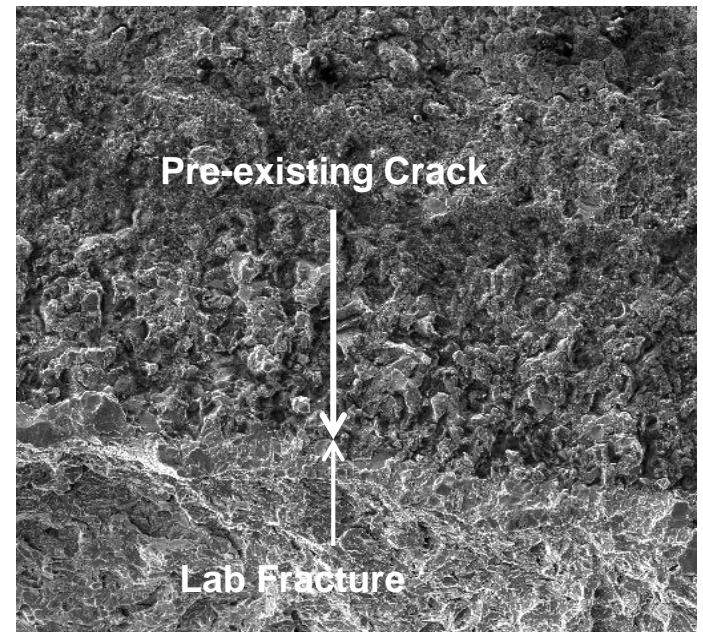
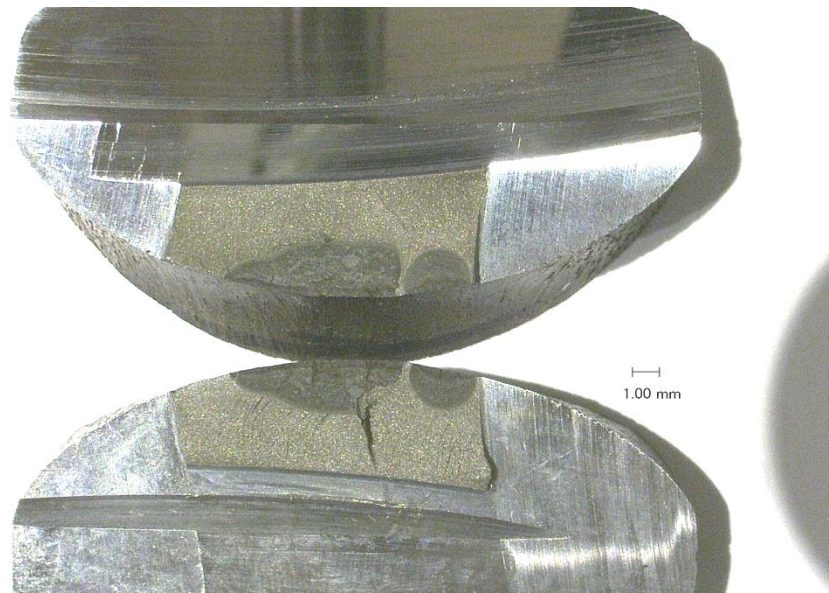
SEM MAG: 50 x
View field: 3.02 mm
Det: SE Detector
HV: 20.00 kV
1 mm
VEGA TESCAN

SEM MAG: 10 x
View field: 14.83 mm
Det: BSE Detector
HV: 20.00 kV
5 mm
VEGA TESCAN

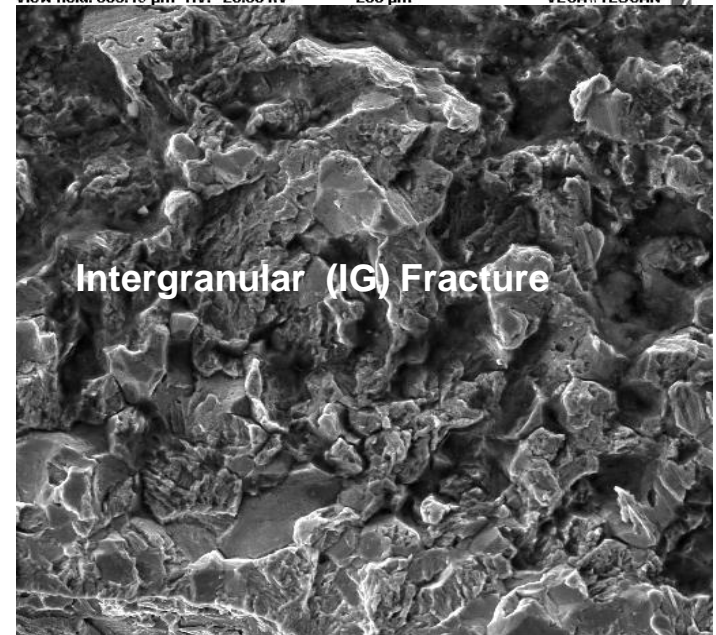
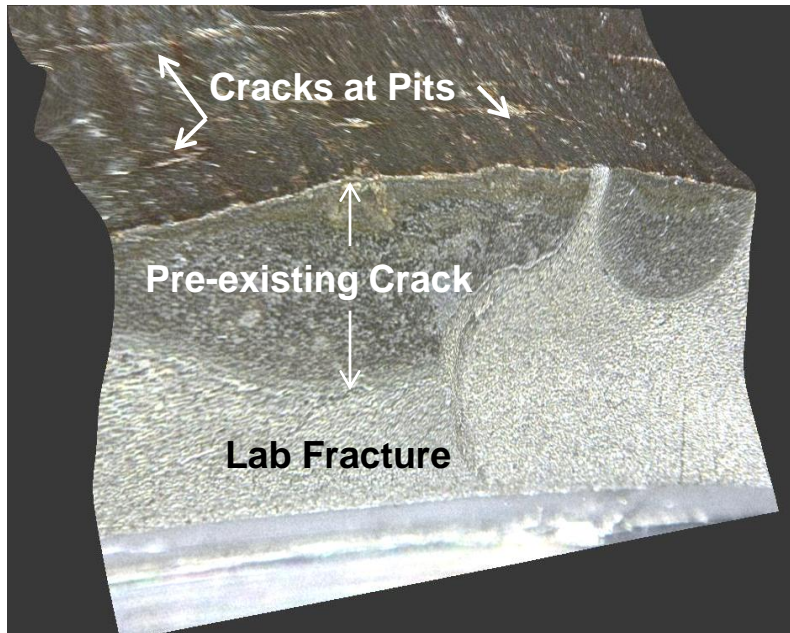


SEM MAG: 1.01 kx
View field: 150.02 µm
Det: SE Detector
HV: 20.00 kV
50 µm
VEGA TESCAN

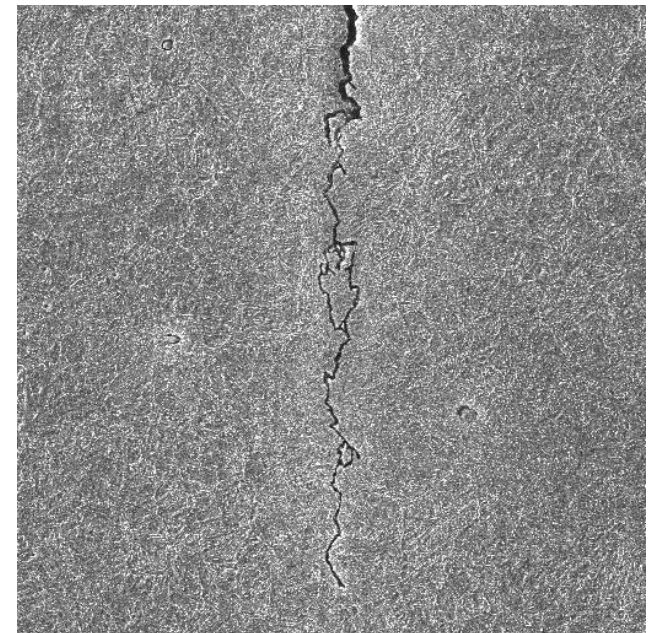
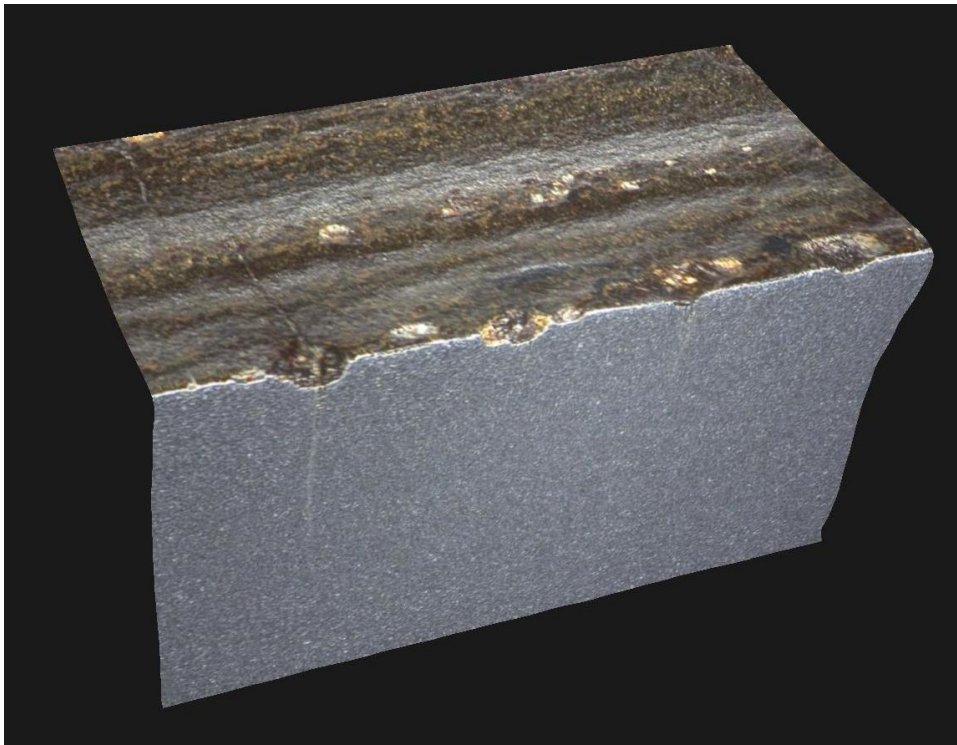
SEM MAG: 100 x
View field: 1.51 mm
Det: BSE Detector
HV: 20.00 kV
500 µm
VEGA TESCAN



SEM MAG: 250 x Det: SE Detector
View field: 603.19 μm HV: 20.00 kV 200 μm VEGA TESCAN



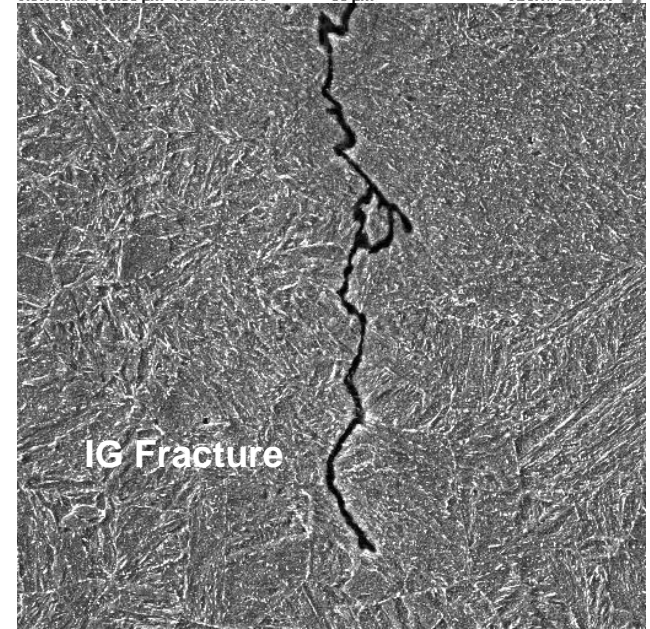
SEM MAG: 1.00 kx Det: SE Detector
View field: 150.80 μm HV: 20.00 kV 50 μm VEGA TESCAN



SEM MAG: 1.00 kx Det: SE Detector
View field: 150.80 μm HV: 20.00 kV



VEGA TESCAN

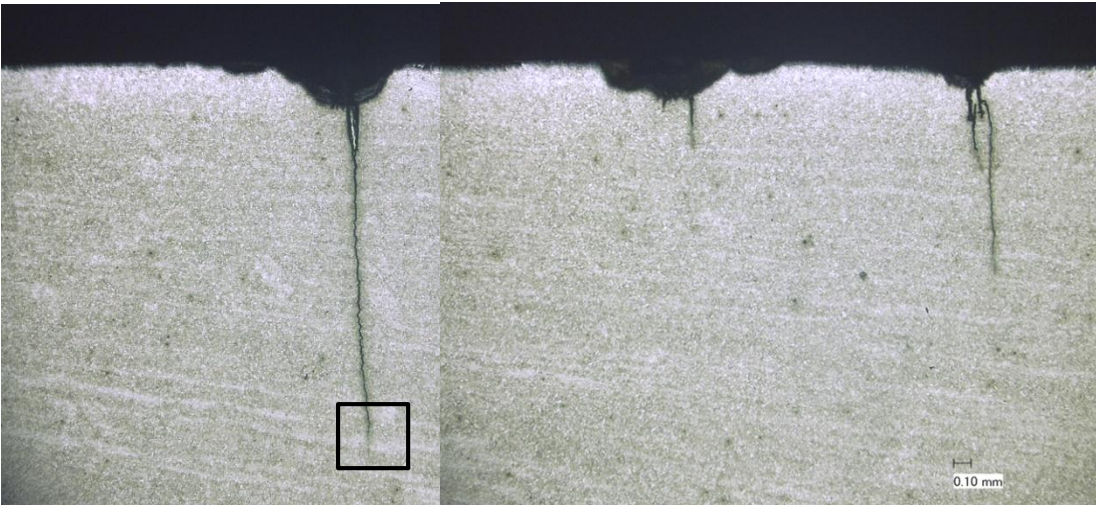


IG Fracture

SEM MAG: 2.50 kx Det: SE Detector
View field: 60.32 μm HV: 20.00 kV



VEGA TESCAN



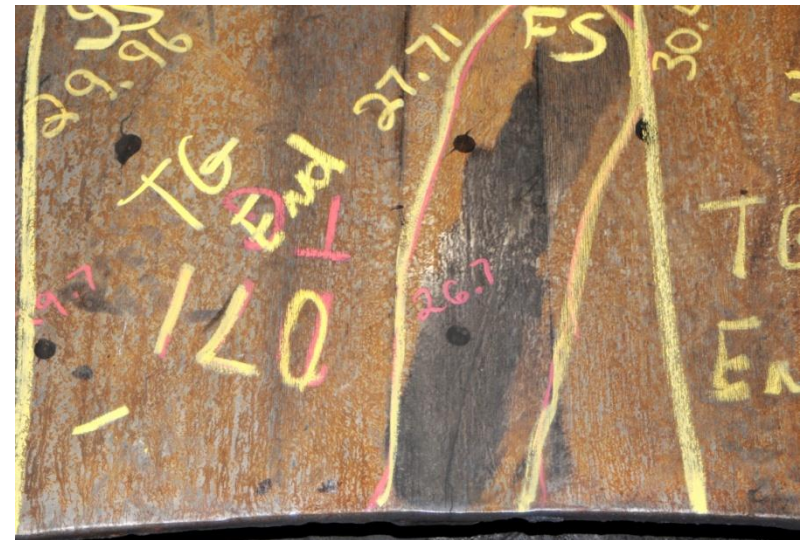
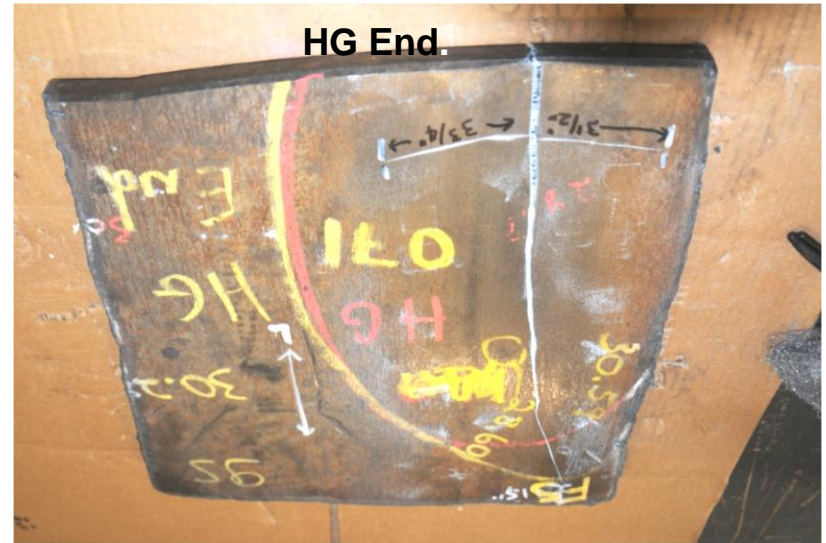
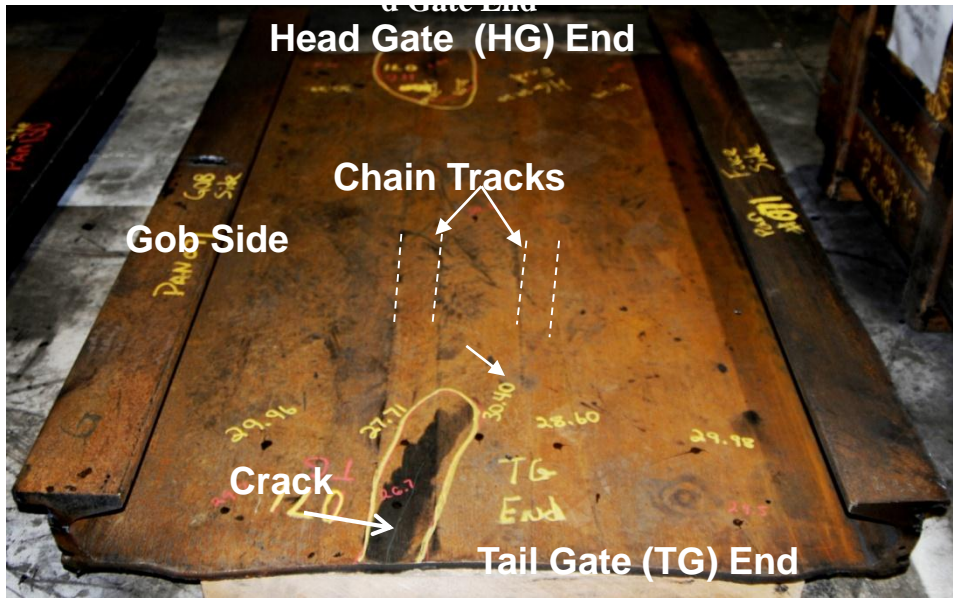
0.10 mm

Analysis of 34 x 110 mm Chain Splice Link – Summary

- Failure was environmentally governed and related to material selection, the environment, and operating conditions.
- Specifically, failure was caused by corrosion fatigue cracks that exhibited multiple initiation sites at corrosion pits on inside surface of links. The cracks propagated completely through the cross section before failure occurred.
- Chemical composition and hardness/strength satisfied the requirements of the governing specifications.
- The ability of the splice link to tolerate a full thickness crack before terminal fracture shows the nominal stresses were low and the material exhibited sufficient toughness for the application.
- Under the same mining conditions, un-galvanized splice links of the same composition and strength level have exhibited satisfactory service performance.

Analysis of Cracks in AFC Pans - Background

- **Armored face conveyor (AFC) had been in service on five (5) panels and had mined approximately 10M raw tons before cracks were detected in the top deck plate.**
- **When the conveyor was fabricated, two (2) grades of abrasion resistant steel was used for the application. One grade was specified to hardness level of ~ 450 HB and the other 500 HB.**
- **Visual examination of pans in a rebuild shop revealed the presence of numerous longitudinal cracks in the top deck plate, most of which were within or immediately adjacent to the chain tracks.**
- **Of the 18 pans included in the investigation, most contained multiple longitudinal cracks.**
- **Crack lengths ranged from 50.8 mm to 1778 mm and were present on both head gate (HG) end, tail gate (TG) end or both ends and gob-side, face side or both sides.**
- **Seven (7) of the pans were selected for detailed analysis (Chemical composition, hardness, tensile and Charpy V-notch impact tests and fractographic/metallographic examinations).**

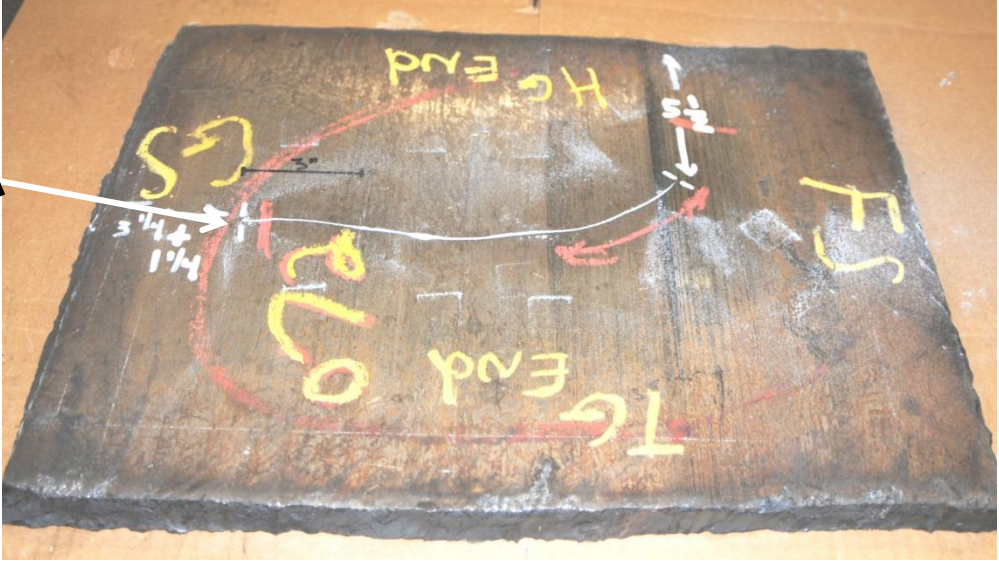


Pan 71 deck plate



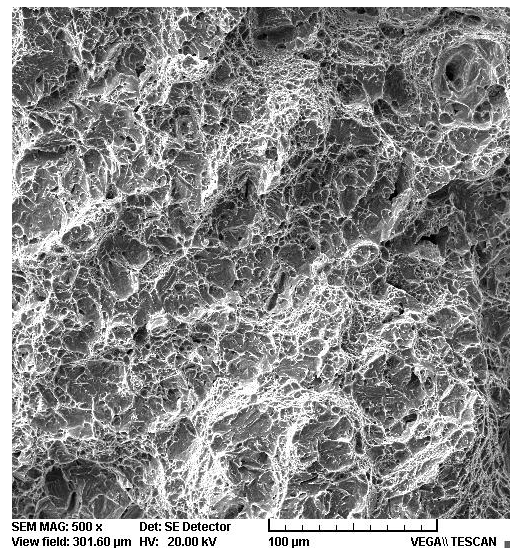
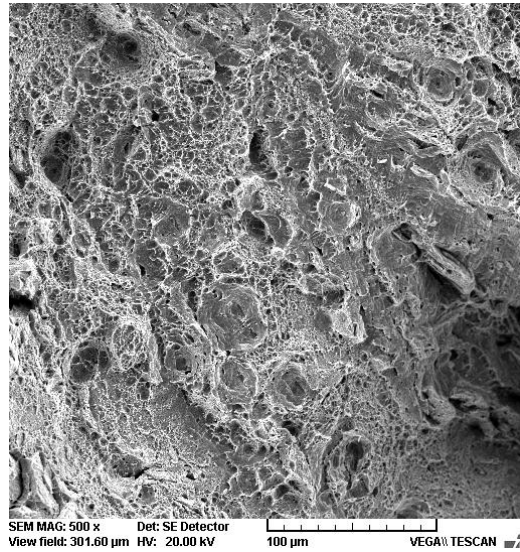
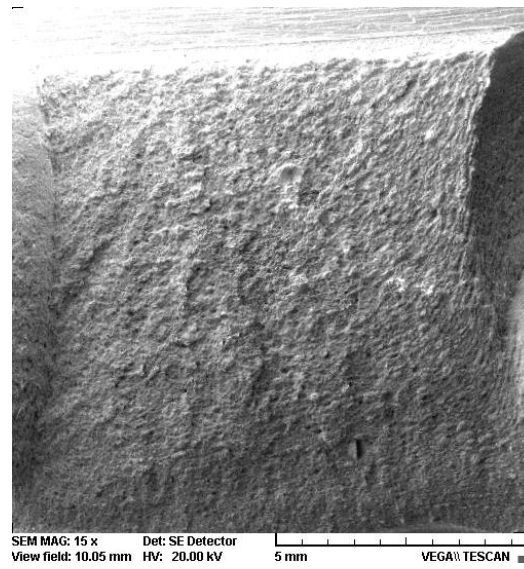
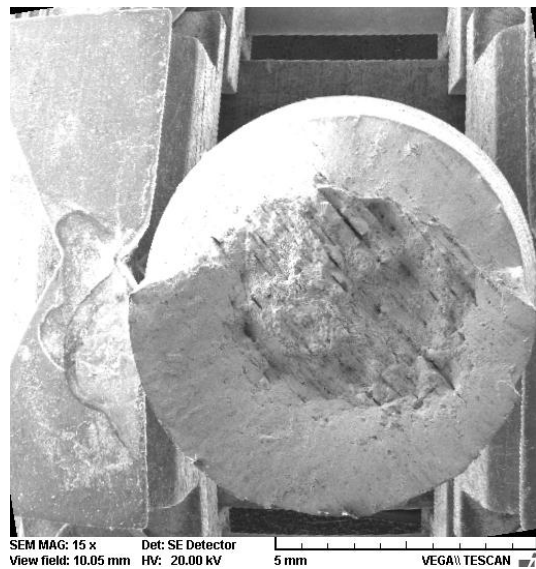
Transverse Crack (intersects both chain tracks)

Pan 72 deck plate



Chemical and Mechanical Properties of Cracked Deck Plates

- Other than hardness/strength, the only significant difference between the 450 HB and 500 HB grade material was carbon content.
- Chemical analysis revealed the deck plate containing the transverse crack (Pan 72) was fabricated from RAEX AR 500 (Finland).
- Results of longitudinal (L) and transverse (T) tensile tests revealed there was no significant difference between the 450 and 500 HB deck or the RAEX 500 HB deck plates.
- Results of L and T CVN impact tests revealed that except for the 500 HB deck plate on Pan 133, which exhibited energy values in the range of 14.5 to 17J (10.7 to 13 ft-lbs), the exhibited CVN absorbed energy values were within the range typical for 450 HB (40J (29.5 ft-lb) and 500 HB 30J (22 ft-lb) plate, respectively.



Pan 71 Tensile Fracture

Pan 71 CVN Impact Fracture

Electron images of Pan 71 tensile and CVN fractures showing the presence of predominantly ductile fracture.



Pan 71 Head Gate



Pan 71 Tail Gate

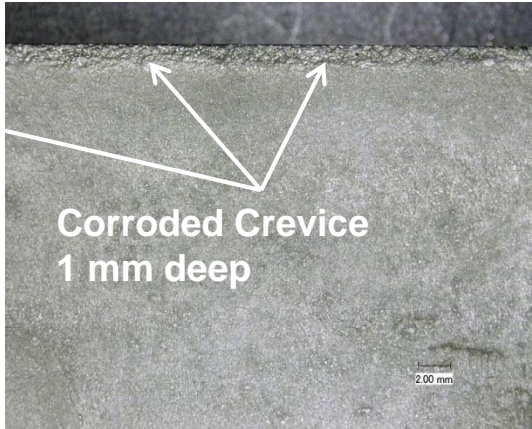
Crack Arrest Marks

Crack Initiation

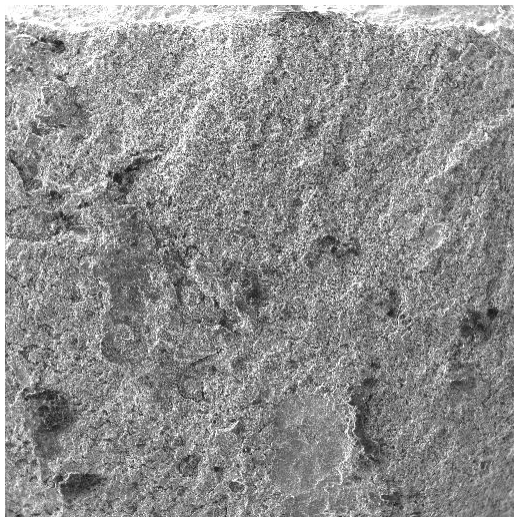


Pan 71 Tail Gate - Opened primary crack.

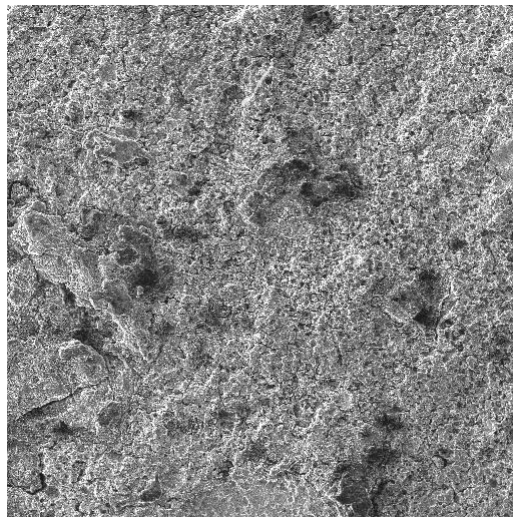
As-opened primary crack – HG end of Pan 71



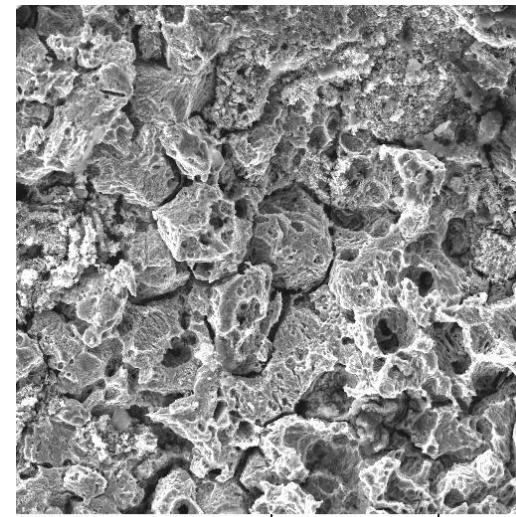
Crack tip of major crack in Head Gate end of Pan 71.



SEM MAG: 50 x Det: SE Detector
View field: 3.02 mm HV: 20.00 kV 1 mm VEGA\TESCAN

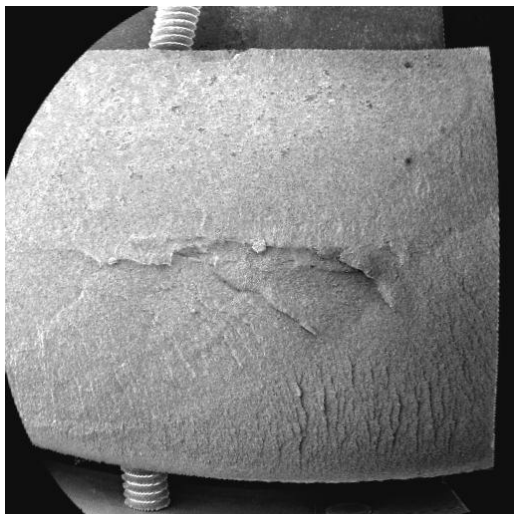


SEM MAG: 100 x Det: SE Detector
View field: 1.51 mm HV: 20.00 kV 500 μm VEGA\TESCAN

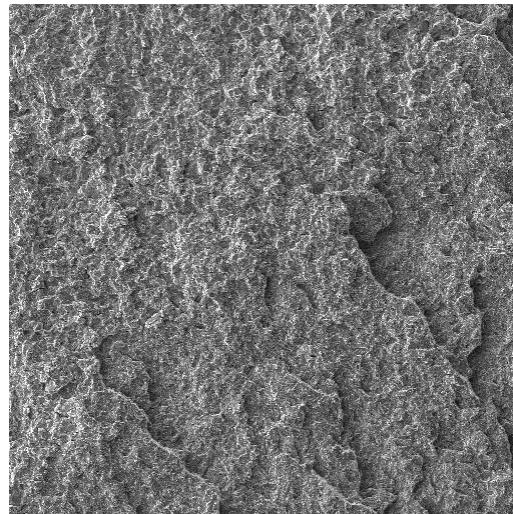


SEM MAG: 1.00 kx Det: SE Detector
View field: 150.80 μm HV: 20.00 kV 50 μm VEGA\TESCAN

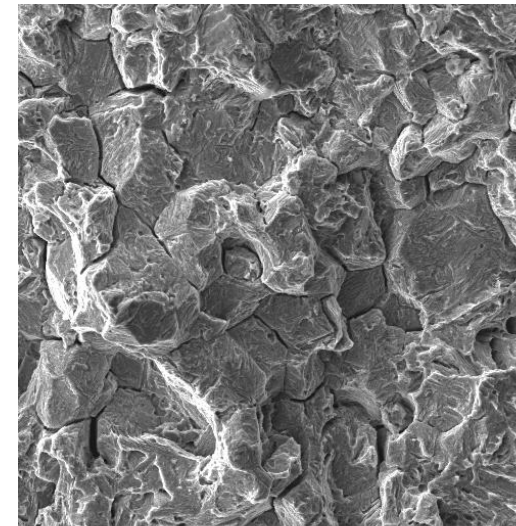
Intergranular fracture near chain contact surface at HG end of Pan 71 deck plate.



SEM MAG: 3.6 x Det: SE Detector
View field: 42.25 mm HV: 20.00 kV 20 mm VEGA\TESCAN

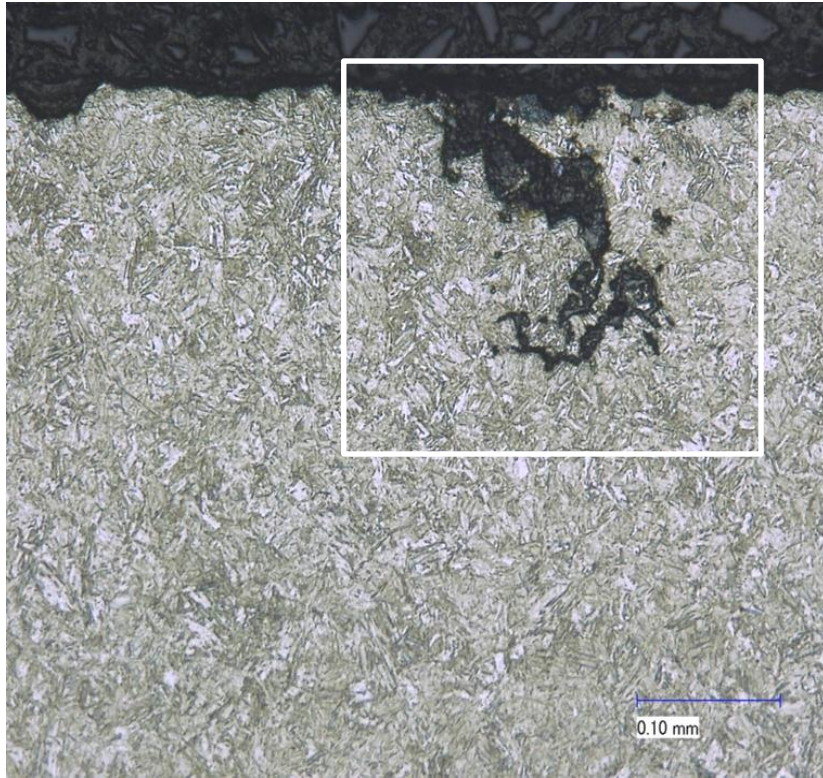


SEM MAG: 100 x Det: SE Detector
View field: 1.51 mm HV: 20.00 kV 500 μm VEGA\TESCAN

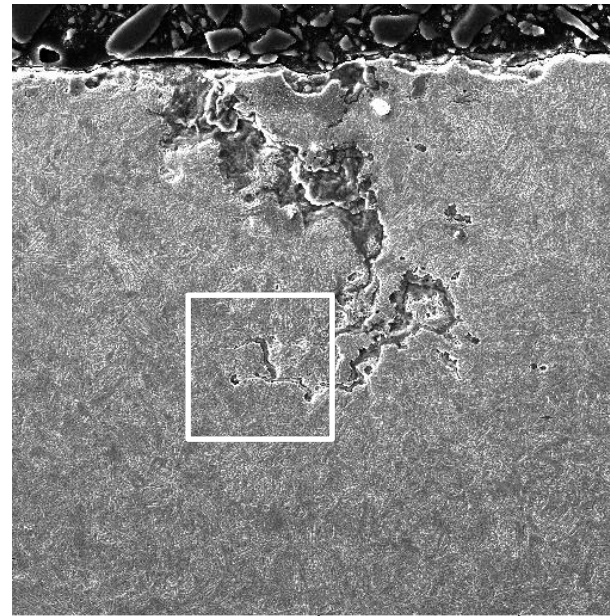


SEM MAG: 1.00 kx Det: SE Detector
View field: 150.80 μm HV: 20.00 kV 50 μm VEGA\TESCAN

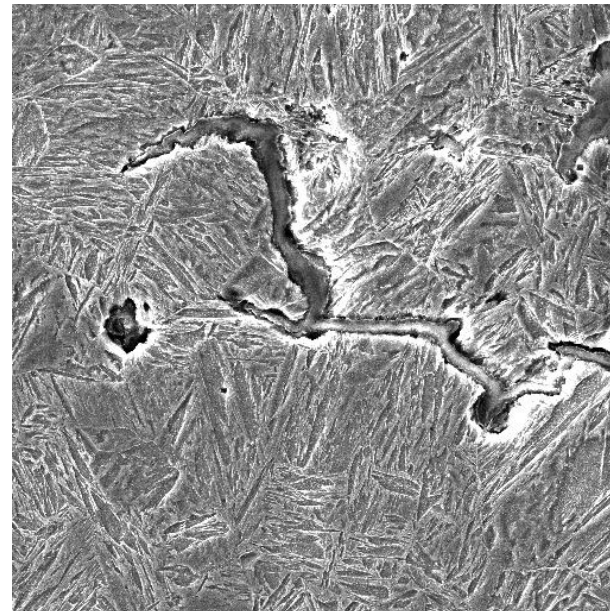
Intergranular fracture at crack tip at HG end of Pan 71 deck plate.



0.16 mm deep IG crack on chain contact surface of Pan 71 deck plate.



SEM MAG: 500 x Det: SE Detector
View field: 301.60 µm HV: 20.00 kV 100 µm VEGA TESCAN



SEM MAG: 2.50 kx Det: SE Detector
View field: 60.32 µm HV: 20.00 kV 20 µm VEGA TESCAN

Analysis of Cracks in AFC Conveyor Deck Plates - Summary

- **Irrespective of plate grade, source, orientation, and mechanical properties, cracks initiated in the chain contact surface of both the 450 HB and 500 HB abrasion resistant plates.**
- **In all cases, fractographic/metallographic examination produced the following conclusions**
 - **The cracking that developed in service was progressive, exhibiting multiple crack arrest markings and intergranular fracture.**
 - **Fracture surfaces of all tensile and CVN impact tests exhibited predominantly ductile fracture.**
 - **As-expected, the cryogenic laboratory fractures exhibited brittle cleavage fracture.**
 - **All deck plates exhibited a uniform martensitic microstructure.**

Analysis of Cracks in AFC Conveyor Deck Plates - Summary

- **Cracking is consistent with both stress corrosion and corrosion fatigue.**
 - **Corrosion fatigue is the combined action of fatigue and corrosion and can produce a failure in fewer cycles and lower loads than if corrosion or fatigue were acting alone.**
 - **Of all corrosion mechanisms, corrosion fatigue is the most difficult to identify, especially in the presence of low-frequency loading.**
 - **At very low frequency loads (i.e. during shear pass or conveyor push), corrosion fatigue can exhibit the same fractographic features as stress corrosion cracking (SCC).**
- **When subjected to wide frequency spectrum, a component can exhibit SCC at low cycles and corrosion fatigue at high cycles.**
 - **Described as corrosion fatigue because of the presence of “beach” marks at the tips of the service induced cracks.**
 - **Highly possible that the “beach” marks are not marking a crack growth cycle, but periods of inactivity → distance between the marks are due to multiple, low stress cycles at low frequency in a corrosive environment. (Marks are not due to a single cycle at high stress.)**

Analysis of Cracks in AFC Conveyor Deck Plates - Summary

- **Many variables affect corrosion fatigue**
 - **Specific combination of material**
 - **Frequency and stress of cyclic loading**
 - **Local environment**
- **Synergistic effect of fatigue and SCC can lead to greater degradation in load carrying capacity than either effect acting alone. Corrosion fatigue can reduce the effective fatigue limit by as much as a factor of 10.**
- **Similar failures have occurred in other equipment built of high hardness/strength abrasion resistant steel that were stored outside. In those cases, fatigue was ruled out because they were not subjected to any external cyclic loads.**
- **These longitudinal intergranular cracks, initiated at micro-cracks in a cut edge, had their SCC propagation governed by the residual stresses induced during fabrication.**